
A BRIEF INTRODUCTION TO SATELLITE COMMUNICATIONS FOR NON-TERRESTRIAL NETWORKS (NTN)

José Alberto Hernández

Universidad Carlos III de Madrid
28911 Madrid, Spain
jahgutie@it.uc3m.es

Pedro Reviriego

Universidad Politécnica de Madrid
28040 Madrid, Spain
pedro.reviriego@upm.es

May 9, 2023

ABSTRACT

At present (year 2023), approximately 2,500 satellites are currently orbiting the Earth. This number is expected to reach 50,000 satellites (that is, 20 times growth) for the next 10 years, thanks to the recent advances concerning launching satellites at low cost and with high probability of success. In this sense, it is expected that next years the world will witness a massive increase in mobile connectivity thanks to the combination of 5G deployments and satellites, building the so-called Space-Terrestrial Integrated Network (STIN), thanks to the emergence of Non-Terrestrial Networks (NTNs). This document overviews the foundations of satellite communications as a short tutorial for those interested in research and development on Space-Terrestrial Integrated Networks (STIN) and Non-Terrestrial Networks (NTN) for supporting 5G in remote areas.

Keywords Satellite Communications (SatComms) · 5G · Non-Terrestrial Networks (NTN)

1 Introduction

In the USA, about 20% of the population lives in rural areas, this accounts for about 97% of the total land. This number grows to 28% in Europe, and about 40% world-wide. In many cases, fiber deployment does not reach rural areas (at least the last mile), since this results very expensive for network operators, hard to justify in terms of Average Revenue per User (ARPU). Indeed, it is estimated that every single meter of fiber connectivity costs approximately 100 US dollars. The largest share of this cost includes digging, trenching and the civil works in general [21]. Satellites can be a good solution to provide broadband connectivity in those areas where fiber cannot reach (deep rural, seaside, desert, mountains, etc).

Indeed, in the past years, the research community has witnessed a race toward deploying different satellite constellations to provide connectivity to both rural and remote areas. This is mainly due to the cost reduction in launching the satellites themselves, approximately a few thousand USD per kg of mass [17] for SpaceX Falcon 9. In this sense, it is estimated that approximately 2,500 satellites are currently orbiting the Earth, a number that is foreseen to grow to 50,000 within ten years [4].

Essentially, while GEO and MEO constellations suffer from high two-way delays, in the order of several hundreds of milliseconds, with subsequent performance degradation of TCP protocols, LEO constellations can further reduce such delays to few tens of milliseconds. Furthermore, High-Altitude Platforms (HAPs) operating at 20 Km distance can even reduce RTTs to few milliseconds.

It is worth noticing that light travels at approximately 300,000 km/s through the air, while it does at 200,000 km/s over silica fiber. That is, the air is 50% faster than silica fibers in terms of propagation delay. This translates into a propagation delay of $3.33 \mu\text{s}/\text{km}$ for free-space communications and $5 \mu\text{s}/\text{km}$ for fiber transmission. In fact, some authors claim that satellite communications can be faster than fiber in wide area scenarios above 1,000 km [10, 11], especially in those regions with difficult conditions for fiber deployment (i.e. desert, mountains, etc).

In particular, a number of companies have focused on deploying Low Earth Orbit (LEO) satellite constellations (between 500 - 1200 km altitude) since latency in these cases are moderate (few tens of milliseconds). In addition to providing coverage to rural areas, satellites can provide connectivity worldwide and are very resilient to natural disasters and wars. LEO satellite constellations can provide sufficient connectivity performance for Machine-Type Communications (MTC) and Mobile Broadband (MBB) in such remote areas [13], paving the way for Non-Terrestrial Networks (NTN) that complement existing Terrestrial Networks, both fixed and mobile. The authors of [8, 9] provide a summary of architectures and challenges to integrate LEO constellations in the 5G ecosystem and even 6G [1]. A detailed survey on this matter is exhaustively studied in [22].

Four major companies are already deploying LEO satellite mega-constellations, namely Telesat, Tesla's Starlink, OneWeb and Amazon Kuiper. The authors in [5] provide a thorough comparison of the LEO constellations and features provided by these four major players, showing tens of milliseconds latency and average throughput in the order of Gb/s per satellite. Vertical applications like rural broadband, IoT applications like smart agriculture and animal tracking, environmental protection and public safety can represent interesting market opportunities to trigger further satellite developments.

This article provides a brief review on the basic principles and design requirements of satellite communications. This review contains several numerical examples to give the reader a better feeling of the uses and applications of satcoms. To this end, Section 2 briefly reviews the most important design aspects of Satellite Communications. Section 3 introduces current mega-constellations and existing projects for NTNs as of year 2023. Finally, Section 4 concludes this work with a summary of its main contributions.

2 An overview of satellite communications

2.1 Orbits and propagation delay

In general Non-Terrestrial Networks (NTNs) refer to networks providing connectivity through space-borne vehicles or airborne platforms, including satellites, High-Altitude Platforms (HAPs) and Low-Altitude Platforms (LAPs). These provide radio connectivity between the User Equipment (UE) on the ground and the vehicle which, in addition, provide connectivity to Terrestrial Networks (TN) through Ground Based Gateways (see Fig. 1).

Depending on the altitude of the space-borne, multiple NTN options are possible:

- Stationary satellites placed in GEO, operating at 35,876 km altitude. GEO scenarios are often equipped with Very High Throughput Satellites (VHTS), providing tens or hundreds of Gb/s capacity each. In this case, Doppler effects are negligible but propagation delays can reach up to several hundreds of milliseconds for transparent satellites.

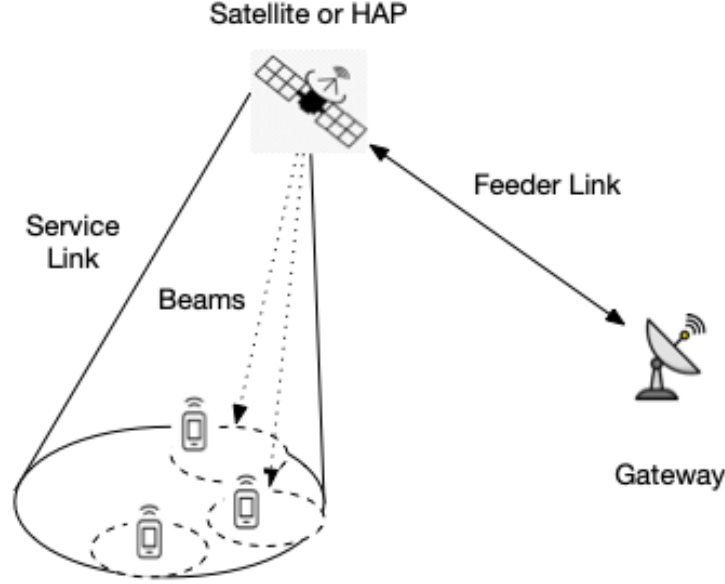


Figure 1: Architecture and terminology.

- Non-stationary satellites positioned in MEO (7,000-25,000 km) or LEO (300-2,000 km), in relative motion to the earth. In these cases, latency values can be moderate, in the range of tens of milliseconds, but Doppler needs compensation. Satellite coverage and their cells may be stationary or not. The former requires the beams fixed on Earth, while the latter simply implies that the beams move at the same speed of the satellites (typically few km/s for LEO sats). In the case of non-stationary cells, methods for handover operations and roaming are required.
- High Altitude Platforms (HAPs) like planes or balloons, operating like satellites but closer to the Earth, at about 20 km distance. HAPs latency values are often below 10 ms.
- Low Altitude Platforms (LAPs) like drones or balloons at less than 1 km altitude.

The altitude of the space-borne has a clear impact on the round-trip time. In this regard, it is worth remarking that latency heavily affects TCP throughput in TCP/IP based networks, which for traditional TCP implementations is given by the Mathis formula [18], further validated in [20]:

$$Throughput_{TCP} < \frac{MSS}{RTT} \frac{C}{\sqrt{p_{loss}}} \quad (1)$$

where MSS is the Maximum Segment Size and RTT is the end-to-end Round-Trip Time; C is a constant that can be estimated from measurements (a number between 1 and 1.5 typically) and p_{loss} is the packet loss probability, due to any factor (packet corruption, collisions in shared media or buffer overflow due to congestion).

Numerical example no. 1: As an example, consider a connection between two cities separated 200 ms, MSS of 1500 Bytes and packet loss probability of 10^{-9} (typical fiber loss) [23]. Substituting in eq. 1, the maximum rate is 1.9 Gb/s (assuming $C = 1$). If latency is doubled (i.e. 400 ms), then the maximum TCP throughput drops to 950 Mb/s. On the other hand, if the packet loss probability is 10^{-6} , then the throughput drops to 30 Mb/s for RTT values of 400 ms. Thus, TCP throughput is heavily affected from both high-latency and unreliable links, especially the latter.

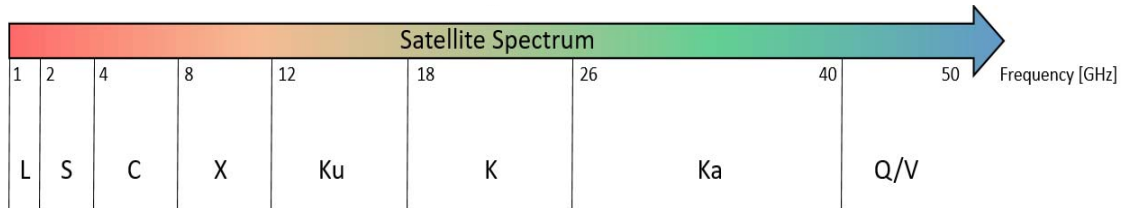


Figure 2: Satellite spectrum [15].

2.2 Frequency bands

Both Fig. 2 and Table 1 summarise detailed information regarding frequency bands allocated by the ITU for satellite communications. As shown, the L and S bands do not offer much bandwidth (tens or hundreds of KHz to few MHz typically) and are often destined to IoT applications with low bandwidth requirements. The Ka and Ku bands provide a lot more bandwidth (tens or hundreds MHz) and can be used to provide Mobile Broadband (MBB) connectivity, similar to those experienced in DSL connections (say 20 Mb/s) even similar to fiber to the home (100 Mb/s and above), especially in cases with high antenna gains. Finally, the Q/V bands offer even larger bandwidth capacity values (hundreds MHz to few GHz) but are more subject to atmospheric losses and absorption from rain. In this regard, some satellite companies are considering the V band for inter-satellite links (ISL) since they are above the clouds, offering mesh connectivity between satellites. Also, some experimental scenarios consider the W Band (between 75-110 GHz) which provides even more bandwidth than the Q and V bands, and should be also used for inter-satellite links (ISL) since this band heavily suffers from propagation impairments and rain fade.

Table 1: ITU Frequency allocations for satellite communications

Sat Band	Downlink (DL)	Uplink (UL)
L band (GEO)	1518 – 1559 MHz	1626.5 – 1660.5 MHz 1668 – 1675 MHz
L band (Non-GEO)	1613.8 – 1626.5 MHz	1610.0 – 1626.5 MHz
C band	3400 - 4200 MHz 4500 - 4800 MHz	5725 - 7025 MHz
S Band	2160 -2200 MHz 2483.5 - 2500 MHz	1980 - 2025 MHz
Ku band	10.7 - 12.75 GHz	12.75 - 13.25 GHz 13.75 - 14.5 GHz
Ka band (GEO)	17.3 – 20.2 GHz	27.0 – 30.0 GHz
Ka band (Non-GEO)	17.7 – 20.2 GHz	27.0 – 29.1 GHz 29.5 – 30.0 GHz
Q/V band	37.5 – 42.5 GHz 47.5 - 47.9 GHz 48.2 - 48.54 GHz 49.44 - 50.2 GHz	42.5 – 43.5 GHz, 47.2 – 50.2 GHz 50.4 – 51.4 GHz

2.3 Link-budget calculations

Classical link budget calculations for satellite communications follow the well-known Friis propagation model, where the power at the receiver antenna P_r (also referred to as signal strength S) is:

$$P_r = P_t \frac{G_t G_r \lambda^2}{(4\pi)^2 d^2} = S \quad (2)$$

where P_{tx} is the transmission power of the transmitting antenna, G_t and G_r are the transmission and reception gain of the two antennas, and λ and d are the transmission wavelength and slant range between the transmitter and receiver in the satellite link. Often, the product $P_t G_t$ is called the EIRP or Effective Isotropic Radiated Power.

The receiving antenna both collects the above signal power S and noise N . The amount of noise collected follows:

$$N = k_B T B_w \quad (3)$$

where k_B is the Boltzmann constant ($1.380649 \times 10^{-23} \text{ m}^2 \cdot \text{kg} \cdot \text{s}^{-2} \cdot \text{K}^{-1}$ or $-228.6 \frac{\text{dBW/K}}{\text{Hz}}$), T is the noise temperature and B_w is the bandwidth of the receiving filter. Often, receiver systems and amplifiers are provided with noise figure (NF) values, which is a classical figure of merit used for both receivers and amplifiers (typically 5 to 9 dB of noise figure values). The noise temperature T can be computed from the noise figure as:

$$T = T_{ref} (10^{\frac{NF}{10}} - 1) \quad (4)$$

where the reference (ambient) temperature T_{ref} is often assumed 290 K (i.e. 16.85 °C).

With these values of signal strength S and noise power N at the receiver, and neglecting interference, the signal-to-noise ratio (SNR) in dB follows [16]:

$$\begin{aligned} SNR &= EIRP \text{ (dBW)} \\ &+ G_r/T \text{ (dBi/K)} \\ &- FSPL \text{ (dB)} \\ &- AtmLoss \text{ (dB)} \\ &- AdLoss \text{ (dB)} \\ &- B_w \text{ (dBHz)} \\ &- K_B \left(\frac{\text{dBW/K}}{\text{Hz}} \right) \end{aligned} \quad (5)$$

where G_r/T is the reception's antenna figure of merit, that takes into account both reception Gain (dBi) and Noise Temperature (Kelvin). As an example, the following list gives an overview of typical terminal equipments and their figures of merit:

- 3GPP Class 3 UE, with 0 dBi antenna gain (linear polarized), 200 mW (i.e. 23 dBm) transmission power and 7 or 9 dB Noise Figure. Assuming $NF = 7 \text{ dB}$ and ambient temperature $T_{ref} = 290 \text{ K}$, the noise temperature is $T = 1163.4 \text{ K}$, and $G_r/T = 0 \text{ dBi} - 10 \log_{10}(1163 \text{ K}) = -30 \text{ dB/K}$ at the receiver.
- Very Small Aperture Terminal (VSAT) with 12 dBi antenna gain (circular), 2 W transmission power and 5 dB Noise Figure. In this case, at the receiver $G_r/T = 12 - 10 \log_{10}(627 \text{ K}) = -16 \text{ dB/K}$ at the receiver.
- IoT devices with 0 dBi antenna gain, 290 K noise temperature and transmission EIRP = 23 dBm. The resulting $G_r/T = -24.6 \text{ dB/K}$ at the receiver.

Concerning FSPL, AtmLoss and AdLoss, these refer to Free-Space Path Loss, Atmospheric Loss (due to gases, rain fade, etc) and any other Additional Loss respectively. FSPL is computed as follows:

$$FSPL = 10 \log_{10} \left(\frac{4\pi df}{c} \right)^2 = 20 \log_{10} \left(\frac{4\pi df}{c} \right) \quad (6)$$

where f is the transmission frequency (as shown in Table 1) and d is the slant range, given by:

$$d = -R_E \sin(\alpha) + \sqrt{R_E^2 \sin(\alpha)^2 + h_s + 2R_E h_s} \quad (7)$$

where R_E refers to the Earth radius (6,371 km), h_s is the satellite height/altitude and α is the elevation angle. The slant range d is the distance from the user device to the satellite and can be often approximated by the satellite's orbit, especially for MEO and GEO satellites:

$$d = \sqrt{h_s^2 + (h_s \tan(\alpha))^2}$$

The atmospheric and additional losses take into account the attenuation due to absorption of different molecules in the atmosphere, mainly oxygen and water. Rain fade and availability, not taken into account in eq. 5 accounts for the attenuation due to traversing clouds, rain, etc, which may reduce the availability of the links below 99%. In this sense, the Crane model is often used to estimate these attenuation values on different weather environments (Tundra, Taiga, Maritime, Continental, etc) [3]. Typically, link budget calculations consider clean sky assumptions (i.e. null attenuation due to rain and fading), but a margin value between 2 and 10 dB is often recommended to compensate from rain fading and other unexpected sources of power loss and attenuation.

Numerical example no. 2: Consider a link between a ground station and a MEO satellite operating at $h_s = 21000 \text{ km}$ with elevation angle $\alpha = 1.2^\circ$ (or 0.021 rad).

In this setting, we can approximate the slant angle with the height of the satellite, that is, $d \approx h_s = 21,000 \text{ km}$ since:

$$d = \sqrt{21,000^2 + (21,000 \tan(0.021))^2} = 21,003 \text{ km}$$

The power transmission of the satellite is 26.6 Watt (or 14.4 dBW) and uses a helix antenna with 13 dBi gain. Assuming that the receiving station is a 3GPP Class 3 User Terminal, then the reception gain is 0 dBi. Finally, the satellite operates in the S band, that is, the center transmission frequency is $f = 2 \text{ GHz}$, that is $\lambda = \frac{c}{f} = 0.15 \text{ m}$.

In linear units:

$$\begin{aligned} G_t &= 10^{\frac{13}{10}} = 19.95 \\ G_r &= 10^{\frac{0}{10}} = 1 \end{aligned}$$

The received power at the terminal for satcoms are typically very small, specially for MEO and GEO satellites. In this case, such received power follows 2:

$$P_r = 26.6 \frac{19.95 \cdot 1 \cdot (0.15^2)}{(4\pi)^2 (21000 \cdot 10^3)^2} = 1.71 \cdot 10^{-16} \text{ W}$$

This satellite link uses the S band for transmission (2 GHz center frequency) and uses 1 KHz of bandwidth (that is, 30 dBHz).

Concerning SNR, the different values in eq 5 are:

$$\begin{aligned} EIRP &= P_{tx} G_T = 10 \log(26.6) + 13 = 27.4 \text{ dBW} \\ G_r/T &= 0 \text{ dBi} - 10 \log_{10}(290 \cdot (10^{\frac{7}{10}} - 1)) = -30 \text{ dB/K} \\ FSPL &= 20 \log_{10} \left(\frac{4\pi(21000 \cdot 10^3)(2 \cdot 10^9)}{3 \cdot 10^8} \right)^2 = 184.9 \text{ dB} \\ AtmLoss + AdLoss &= 9.6 \text{ dB} \\ B_w &= 10 \log_{10}(10^3) = 30 \text{ dBHz} \\ K_B &= -228.6 \frac{\text{dBW/K}}{\text{Hz}} \end{aligned}$$

Numerical example no. 2 cont: Hence, the Signal-to-Noise ratio follows:

$$SNR = 27.4 + (-30) - 184.9 - 9.6 - 30 - (-228.6) = 1.5 \text{ dB}$$

or $snr = 10^{\frac{1.5}{10}} = 1.41$ in natural units; that is, the signal power is 41% greater than the noise power at the receiver. This translates into a maximum spectral efficiency (SE) or β_{max} of:

$$\beta_{max} = \log_2(1 + snr) = 1.27 \text{ bps/Hz}$$

This is further explained in the next section.

2.4 Bitrates, Shannon’s capacity limit and Adaptive Coding and modulation

After a given SNR is obtained from the link-budget analysis following eq. 5, this value together with the bandwidth used for transmission provides an upper bound of the maximum achievable bit rate R_{max} , as it follows from the Shannon-Hartley’s theorem:

$$R_{eff} < R_{max} = B_w \cdot \log_2(1 + snr) = B_w \cdot \beta_{max} \tag{8}$$

where the effective bitrate R_{eff} used in transmission cannot be larger than the Shannon’s limit R_{max} .

The value $\beta_{max} = \log_2(1 + snr)$ (in bps/Hz) is often referred to as spectral efficiency (SE) and measures how much bitrate can be obtained from a given bandwidth. Also:

$$\beta_{eff} < \beta_{max} = \log_2(1 + snr) \tag{9}$$

Typical spectral efficiency values range between 0.5 and 2 bps/Hz, reaching even up to 4 bps/Hz in some specific scenarios. Above 5 bps/Hz is often very difficult to achieve in satcoms, unless they are very close to Earth.

Numerical example no. 3: In the previous satcom link (1 KHz of bandwidth), the maximum achievable capacity follows:

$$R_{max} = B_w \log_2(1 + snr) = 1 \cdot 10^3 \log_2(1 + 10^{\frac{1.41}{10}}) = 1.27 \text{ Kb/s}$$

Taking the Shannon’s limit the other way around, the communications link must provide sufficient SNR above the minimum required for a given spectral efficiency:

$$snr_{eff} > snr_{req} = 2^{\beta_{max}} - 1 \tag{10}$$

It is often recommended that a designed SNR provides a margin of a few dB above the Shannon’s limit SNR_{req} as a rule of thumb, to account for unexpected situations with SNR drop (atmospheric conditions, etc).

Ideally, in the case of absence of noise, the spectral efficiency β would only depend on the modulation used, its coding and reception filter roll-off. However, in the presence of noise, each modulation and coding scheme provides a different spectral efficiency as long as a minimum SNR is guaranteed. Table 2 shows the SNR requirements to achieve Quasi-Error Free (QEF) for some classical modulation and coding schemes (MODCOD) used in satellite links [2]. As shown, low-order modulations like APSK are less efficient in terms of bits/symbol than higher-order ones, but their SNR requirements are also smaller. Here, QEF refers to only 2 errors for every 10,000 transmitted bits after Viterbi decoding (i.e. $BER = 2 \cdot 10^{-4}$).

Typically, modems have a wide range of available modulation and coding (MODCOD) schemes that can be used depending on the SNR link budget, which can be dynamically adjusted depending on the conditions of the satellite link.

Table 2: MODCOD table for a theoretical DVB modem, based on Shannon's limit [2]

MODCOD	SE (bps/Hz)	SNR for QEF (dB)
APSK 1/2	0.4	-2
CPSK 1/4	0.5	0
CPSK 1/2	0.6	1
CPSK 3/4	0.65	2
DPSK 1/4	0.75	3
DPSK 1/2	0.9	4
DPSK 3/4	1.05	6
DPSK 5/6	1.25	7
DPSK 7/8	1.5	9

Numerical example no. 4: As an example, consider we want to design a MODCOD scheme for the previous satcom link, where the SNR obtained was 1.41 dB. Looking at Table 2, CPSK 1/2 requires a minimum SNR of 1 dB, and we have 0.41 dB as margin. This MODCOD scheme offers a spectral efficiency of 0.6 bps/Hz which is much smaller than the maximum theoretical value given by the Shannon-Hartley ($\beta_{max} = 1.27$ bps/Hz). Thus, the effective bitrate achieve with quasi-error free (QEF) performance is $0.6 \cdot 1$ Kb/s = 600 bps.

2.5 Increasing capacity with multiple beams per satellite and frequency reuse

At present, at least four major private companies (Amazon Kuiper, Oneweb, Telesat and Starlink) are in the process of deploying large LEO satellite constellations with hundreds (even thousands) satellites at few hundred km above Earth surface. Some of the features of these four mega-constellations are explained in [14] and summarised in Table 3.

Table 3: Constellations for Starlink, Kuiper and Telesat [14]

	Shell	Height (km)	Orbits	Sats/orbit	inclination α
Starlink	S1	550	72	22	53°
	S2	1,110	32	50	53.8°
	S3	1,130	8	50	74°
	S4	1,275	5	75	81°
	S5	1,325	6	75	70°
Kuiper	K1	630	34	34	51.9°
	K2	610	36	36	42°
	K3	590	28	28	33°
Telesat	T1	1,015	27	13	98.98°
	T2	1,325	40	33	50.88°

The footprint area A_{sat} covered by one single satellite follows:

$$D_{sat} = \frac{P_{Earth}}{N_{orbit}} \quad (11)$$

where P_{Earth} and N_{orbit} are the Earth perimeter (40,075 km) and number of satellites per orbit respectively.

Numerical example no. 5: Consider Shell S1 of Starlink, with 22 satellites per orbit. This means that each satellite covers a diameter of:

$$D_{sat} = \frac{40,075 \text{ km}}{22} = 1821.6 \text{ km of diameter}$$

The area/footprint covered per satellite is then:

$$A_{sat} = \pi \left(\frac{D_{sat}}{2} \right)^2 = 2.6 \cdot 10^6 \text{ km}^2$$

Since the total Earth surface is $Su_{Earth} = 510.1 \cdot 10^6 \text{ km}^2$, then the 22 sats cover only 11% of the total Earth surface. Shells S2-S5 should cover the rest of the Earth.

Each LEO satellite is often equipped with multiple antenna beams pointing at different regions (or cells) in its footprint area, and allowing frequency reuse like in mobile networks. This can be achieved in multiple ways, a typical one is by using phased array antennas with high directivity. Indeed, High or Very-High Throughput Satellites (HTS/VHTS) represent an evolution of satellites towards higher capacity through more spot beams and higher frequency reuse. These, applied in LEO orbit constellations, can further provide high bandwidth and reduced latency to enable Mobile Broadband (MBB) and Machine-Type Communications (MTC) in places where both fibre and 5G connectivity has limitations (deep rural areas, sea-side, mountains, etc). V/HTS can be identified by two key technological features [7]:

- The use of multiple spot beams (tens, even hundreds) of narrow beams covering a small geographical area cells, as shown in Fig. 1.
- The frequency reuse of allocated bandwidth in non-adjacent beams/cells, thus higher throughput of the satellite.

Indeed, more capacity can be provided to a given region by partitioning it into smaller sub-regions or cells covered by individual spot beams and leveraging frequency reuse. In this sense, capacity can scale up in the same way as in mobile networks by re-using multiple times the same frequency on non-adjacent cells, while keeping the the Signal to Noise and Interference Ratio (SINR) under acceptable limits for digital communications. Thus, the total satellite capacity R_{tot} increases with the number of beams and polarizations as:

$$R_{tot} = \beta B_w \left(\frac{N_p N_b}{N_c} \right) \cdot (1 - \eta_{guard}) \quad (12)$$

where N_p stands for the number of polarizations (1 or 2), N_b is the number of spot beams (several tens, even hundreds for VHTS), N_c is the number of colors or frequencies (3, 4 or 6 typically), and η_{guard} is the guard-band between sub-bands (often a value between 5 – 10%).

Numerical example no. 6: Consider a satellite operating in the Ku-band with 1.5 GHz bandwidth and spectral efficiency of 2 bps/Hz. Under the assumption of 2 polarizations, 7 colors and 60 spot beams, the total capacity delivered by this satellite in the service link is up to:

$$R_{tot} = 2 \cdot 1.5 \cdot 10^9 \frac{2 \cdot 60}{7} \cdot 0.9 = 46 \text{ Gb/s}$$

Indeed, in the Ku and Ka bands, bandwidth values per spot beam of 1.5-2 GHz are possible. The largest Ka-band satellites are Jupiter-2 and ViaSat-2, offering total aggregate capacity values of 200 to 300 Gb/s.

However, it is worth remarking that using multiple spot beams on-board heavily increases the size and weight of the satellite. For instance, a one hundred spot beams may account for 2,000 Kg of mass [19]. As a rule of thumb, one Kg of weight can cost around 1,000 USD to get it in the sky¹. In this light, scaling HTS satellites to VHTS is cost effective

¹"Launch costs to low Earth orbit, 1980-2100", <https://www.futuretimeline.net/data-trends/6.htm>, last access February 2023

since the cost per Gb/s decreases following a power-law in these types of satellites, empirically [7]:

$$Cost = 167.3 \cdot (R_{tot})^{-0.886} \quad (13)$$

In general, when using multiple beams, each single beam may interfere with adjacent ones in the frequency of operation. The final Signal to Interference and Noise Ratio (SINR) is obtained from combining both noise and interference as:

$$SINR = \frac{S}{N + I} = \frac{1}{\frac{1}{SNR} + \frac{1}{SIR}} \quad (14)$$

Thus, the network designer must be careful at balancing both noise and interference to not reach important signal degradation.

Essentially, the antennas are often designed with high directivity to well illuminate a given cell, while the sidelobes that may appear in neighbouring cells are well below the main lobe, typically 10 dB lower or above. In this sense, a given cell may receive power from other interfering cells, but such interfering power should be very low.

Numerical example no. 7: For instance, consider a LEO sat illuminating a cell with SNR = 9 dB (i.e. the signal is 8 times stronger than the noise power). In this cell, the SIR observed from other interfering cells is only 6 dB (i.e. the signal power is 4 times stronger than the interfering adjacent signals). Then, the combined SINR reduces to 2.67 times or 4.25 dB:

$$SINR = \frac{1}{\frac{1}{9} + \frac{1}{8}} = 2.67 \text{ or } 4.25 \text{ dB}$$

However, if the SIR is 12 dB, then the new SINR becomes 5.14 dB (from SNR = 9 dB).

2.6 Phased Array antennas, radiation pattern and directivity

To achieve highly directive antennas on board, the use of linear or planar phased arrays of N elements is often considered [6]. As an example, consider the Equally-Space Linear Array (ESLA), where N array elements are separated by some distance d , for a total distance of $D = (N - 1)d$. In this case, the Array Factor (AF) follows:

$$AF_{ESLA}(\psi) = e^{j(N-1)\frac{\psi}{2}} \frac{\sin\left(N\frac{\psi}{2}\right)}{\sin\left(\frac{\psi}{2}\right)} \quad (15)$$

where $\psi = kd \cos(\theta)$; here the array is considered to receive signal from a plan wave incident at angle θ to the plane of the array. It is worth remarking that an isotropic antenna has $AF = 1$.

The maximum value of AF occurs when $\psi = 0$, resulting in $AF = N$, which is the directivity of this type of antenna:

$$D_{ESLA} = N \quad (16)$$

Hence, disregarding the phase factor $e^{j(N-1)\frac{\psi}{2}}$ and normalising, we obtain:

$$f(\psi) = \frac{\sin\left(N\frac{\psi}{2}\right)}{N \sin\left(\frac{\psi}{2}\right)} \quad (17)$$

which can be used to plot the radiation pattern and find the area of a cell covered by a beam constructed with an ESLA. Fig. 3 shows examples of AF for different values of N .

As the number of array elements N increases, the width of the main lobe in the radiation pattern decreases, making antennas more directive (with higher gain and smaller area covered). Also, as N increases, the sidelobe level (SLL) decreases, producing less interferences on adjacent cells. For example, for $N = 5$ and $d = \frac{\lambda}{2}$, the directivity of this array is $D_{ESLA} = N = 5$ while the side lobes are very low (see Fig. 4). A metric of interest is the Half-Power

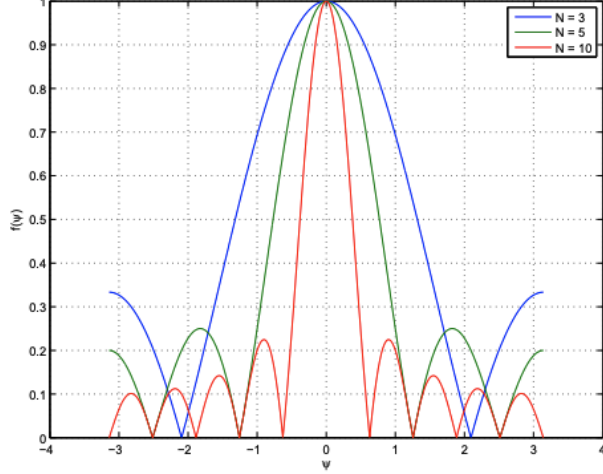


Figure 3: Plots of $|f(\psi)|$ for various N [12].

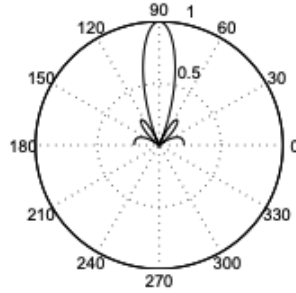


Figure 4: Radiation pattern for $N = 5$ and $d = \frac{\lambda}{2}$ [12].

Beam Width (HPBW) that gives the angle at which the main lobe drops to one half (or 3 dB less directivity than the maximum).

Other arrays than ESLA have different properties and radiation patterns. For instance, Planar Rectangular Arrays (PRA) with N elements again $\lambda/2$ spaced, have a maximum directivity of:

$$D_{PRA} = N\pi \tag{18}$$

The gain of an antenna is typically smaller than its directivity by a factor k_{ef} smaller than one:

$$G = k_{ef}D \quad \text{or} \quad G = D + 10 \log_{10}(k_{ef}) \tag{19}$$

where efficiency $k_{ef} = \frac{P_{rad}}{P_{in}}$ accounts for the ratio of power effectively radiated to the air P_{rad} divided by the input power to the antenna P_{in} . That is, not all incoming power into the antenna is transformed into radiation, part of it is lost; such loss is represented by k_{ef} , and is typically between 0.5 to 0.9. Remark that a value of $k_{ef} = 0.5$ translates into a 3 dB difference between Gain and directivity, as noted in Eq. 19.

It is worth remarking that Gain is relative to isotropic radiation, making the effective aperture of a given antenna proportional to its gain:

$$A_e = \frac{\lambda^2}{4\pi} G \tag{20}$$

The ideal isotropic antenna radiates equally in all 3D directions, therefore it has no gain ($G = 1$ in linear units or $G = 0$ dBi).

In general for planar arrays, the directivity and the HPBW are related by the following approximation:

$$D \approx \frac{32,400}{\theta_{HPBW_{1d}}\theta_{HPBW_{2d}}} \tag{21}$$

where $\theta_{HPBW_{1d}}$ and $\theta_{HPBW_{2d}}$ are the angles (in degrees) where power drops 3 dB (or one half).

Table 4: Directivity and HPBW for different Phased Array antenna configurations

Antenna	Directivity	HPBW
Isotropic	1 (or 0 dBi)	-
Linear $N = 3$	3 (or 4.7 dBi)	104°
Linear $N = 7$	7 (or 8.4 dBi)	68°
Linear $N = 11$	11 (or 10.4 dBi)	54°
Planar 4×4	16π (17 dBi)	25°
Planar 8×8	64π (or 23 dBi)	12.7°
Planar 16×16	256π (29 dBi)	6.4°
Planar 32×32	1024π (35 dBi)	3.2°

Table 4 shows some examples of linear and planar arrays directivity and HPBW for different number of elements N . All cases assume untapered phased arrays, that is, uniformly weighted. As shown, narrow-beam antennas can also achieve high directivity and gain, but require phased arrays with multiple radiating elements.

Numerical example no. 8: Consider the case of a LEO satellite operating at 500 km altitude, willing to have on board multiple antenna beams, each beam covering an area of $7,854 \text{ km}^2$ (that is, a circle with radius $R_{cell} = 50 \text{ km}$ or 100 km of diameter). Then, the HPBW of the antenna to illuminate that area should be:

$$HPBW = 2 \tan^{-1} \frac{R_{cell}}{h_s} = 2 \tan^{-1} \frac{50}{500} = 0.2 \text{ rad or } 11.4^\circ$$

Thus, looking at Table 4, the designer decides to employ an 8x8 Planar Array antenna. Such an antenna has a directivity of 23 dBi on the center of the cell, and 3 dB less at the borders, i.e 20 dBi. Such antenna gain can be used in the Friis equation 2 to dimension the satellite link and further obtain the SNR and spectral efficiency of the link.

Indeed, the directivity of the beams play an important role to properly cover its cell and not interfere adjacent ones where the same frequency is reused. Directivity increases with the number of antenna elements N , but also Side-Lobe Levels (SLL) reduce as N grows, thus producing less interference in neighbouring cells. For instance, the SLL for a linear array with $N = 3$ elements is 0.35 (i.e. -5 dB), while for $N = 10$ is 0.22 (i.e. -6.6 dB). Typical SLL in modern phased arrays with high directivity often start on -10 dB onwards, thus limiting the interference contribution SIR to neighbouring cells.

3 An overview of ongoing satellite constellations for Non-Terrestrial Networks

In this section, we briefly overview some of the characteristics of ongoing NTN projects, including technical aspects like link budget, spectral efficiency, bandwidth and bitrate. More details can be found in [13].

3.1 Thales Alenia Space: LEO constellation

This project is intended to provide land-mobile connectivity to users (pedestrians walking, 3 km/h) in North America. The satellite antenna has 34 dBW/MHz of EIRP density and G/T of 1.1 dB/K while in the ground, pedestrians have a terminal class 3GPP class 3 UE.

The following is a list of its main features:

- Orbit: LEO at 600 km
- Elevation angle: 30°
- Frequency reuse: 3
- S-band: 2 GHz both uplink and downlink
- Bandwidth: 10 MHz downlink and 360 KHz uplink
- SINR: 5.5 dB in downlink and 2.5 dB uplink
- SE: 1.35 and 1 bps/Hz in downlink and uplink respectively
- Bitrate: 13.5 Mb/s and 360 Kb/s DL and UL respectively.

3.2 Intelsat HAPs

This project is intended to provide connectivity to deep rural areas in Nigeria using HAPs at nominal altitude of 20 ± 2 km (50 ms approx) covering a fixed area on Earth of 50 km radius (that is 7855 km²). The number of antenna beams on board is 16, hence each beam covers a cell of radius R_{cell} as follows:

$$A_{cell} = \frac{A_{HAP}}{16} \Rightarrow \pi R_{cell}^2 = \frac{\pi R_{HAP}^2}{16}$$

Thus:

$$R_{cell} = \sqrt{\frac{R_{HAP}^2}{16}} = 12.5 \text{ km}$$

Regarding users on ground, these are considered to follow 3GPP Class 3 UE (that is, 0 dBi antenna gain and 9 dB NF in reception and 23 dBm of EIRP in transmission).

Other important parameters of this NTN include:

- Orbit: HAPs (18-22 km altitude)
- S-band: 1.8 GHz
- Bandwidth: 13 MHz both DL and UL
- SINR: about 21 dB in the center of cell and between 2 and 7.9 dB at the border.
- Link margin: 4 dB for rain fade.
- SE: 5.555 bps/Hz for DL and between 0.8 and 1.4 bps/Hz in UL.
- Bitrate: 72 Mb/s for DL and between 10 and 18 Mb/s in UL.

3.3 Inmarsat GEO IoT

This GEO project was conceived for IoT applications (NB-IoT standard) in Algeria, where latency is not critical and the IoT applications do not have important bandwidth requirements. The following list shows some of its main features:

- Orbit: GEO (38,000 km altitude)
- L-band: 1.5 GHz
- Bandwidth: 200 KHz for DL and 15 KHz for UL
- SINR: not provided
- SE: 0.67 bps/Hz for both DL and UL respectively.
- Bitrate: 112 Kb/s to 9.33 Kb/s in DL and UL respectively.

3.4 Echostar GEO

In this project, GEO satellites offer land-mobile and broadband connectivity to rural areas in both Africa and America. Two user equipments are possible: 3GPP Class 3 UE and VSATs for better SINR, allowing higher bitrates. Some of its main features include:

- Orbit: GEO (38,000 km altitude)
- S-band: 2 GHz
- Frequency reuse: 3
- Bandwidth: Not specified.
- SINR: 15.4 dB and 11 dB in DL and UL respectively for VSATs, and 3 and 0.7 dB for Class 3 UE.
- SE: 4 and 2.5 bps/Hz for both DL and UL respectively for VSATs, and 1.2 and 1.0 bps/Hz for Class 3 UE.
- Bitrate: Not specified.

3.5 OneWeb LEO

In this project, LEO satellites offer both ubiquitous connectivity and high-capacity worldwide, allowing seamless integration with terrestrial networks. Flat pannel antennas are considered on the ground for better G/T (between 7 and 9 dB)

- Orbit: LEO 1,200 km
- S-band: Ku (11.7 GHz DL and 14.5 GHz UL)
- Atmospheric loss: 2 dB margin
- Bandwidth: Not specified.
- SINR: Not specified.
- SE: Not specified
- Bitrate: 830 Mb/s symmetrical in best case, 140 Mb/s worst case.

3.6 Intelsat GEO HTS

In this project, a GEO High-Throughput Satellite (HTS) operating in the Ku band is considered for its use to provide broadband to maritime scenarios in the Mediterranean Sea. VSAT antennas with high G/T values on ground are considered.

- Orbit: GEO (38,000 km altitude)
- Ku-band
- Number of beams: hundreds to thousands
- Bandwidth: Not specified.
- SE: 0.6 bps/Hz in DL and 1.6 bps/Hz in UL worst case (beam edge); 1 and 1.6 bps/Hz respectively as best case.
- Bitrate: Not specified.

3.7 Avanti GEO HTS

In this project, a GEO HTS is conceived to provide connectivity for connected cars in Western Europe or North America. The car is considered to have on board an antenna with large G/T of 7.4 dB/K.

- Orbit: GEO (38,000 km altitude)
- Ka-band
- Bandwidth: Not specified.
- SINR: 2.3 and 4.4 in DL and UL respectively, under clear sky considerations.
- SE: 0.9 and 1.3 bps/Hz as best case.
- Bitrate: Not specified.

3.8 Hispasat Amazonas 3 GEO

In this project, several satellites (Amazonas 1, 2, 3 and subsequent) have been launched on GEO orbit to provide connectivity both in rural areas and maritime applications. Some of its features are:

- Orbit: GEO (35,786 km altitude)
- Ka, Ku and C band
- Number of beams: 63 transponders (9 for user and 4 for gateway in Ka band, 33 in Ku band and 19 in C band).
- Bandwidth: 54 MHz (Ku and C) and 36 MHz (Ku and C).
- SINR: Not specified.
- SE: Not specified
- Bitrate: Between 30 and 60 Mb/s.

3.9 Summary table

Table 5 shows a summary of the main features of the previous on-going NTN projects.

Table 5: Use cases and demonstration scenarios of [13]

Contributor	Orbit	freq	BW	SINR (DL/UL)	SE (DL/UL)
Thales	LEO	S (2 GHz)	10/0.36 MHz	5.5/2.5 dB	1.35/1 bps/Hz
Intelsat	HAPS (18-22 km)	S (1.8 GHz)	13/13 MHz	13 dB	2.2/2.4 bps/Hz
Inmarsat	GEO IoT (38,000 km)	L (1.5 GHz)	200/200 KHz	NA	0.6-1.33 bps/Hz
EchoStar	GEO 38,000 km	S (2 GHz)	NA	15(3)/11(0.7)* dB	4/1.2 bps/Hz
OneWeb	LEO 1,200 km	Ku	NA	140 to 830 Mb/s	4/1.2 bps/Hz
Intelsat	GEO HTS	Ku	NA	0.5-1.9 9 dB dB	0.6-1.9 bps/Hz
Avanti	GEO HTS	Ka	NA	2.3/4.4 dB	0.9/1.3 bps/Hz

4 Discussion and future work

This article has briefly overviewed the use of satellites and HAPs for providing connectivity in those areas where fiber cannot reach, namely deep rural areas, mountains, desert and seaside. The foundations regarding link budget analysis and achievable bitrates are also reviewed, along with an introduction to antenna array systems and cellular designs.

Finally, some of the most popular emerging satellite constellations and HAP projects are briefly reviewed, along with their characteristics and limitations.

Funding

The authors would like to acknowledge the support of project 6G-INTEGRATION-3 (grant no. TSI-063000-2021-127), funded by UNICO-5G program (under the Next Generation EU umbrella funds), Ministerio de Asuntos Económicos y Transición Digital of Spain.

References

- [1] Giuseppe Araniti, Antonio Iera, Sara Pizzi, and Federica Rinaldi. Toward 6g non-terrestrial networks. *IEEE Network*, 36(1):113–120, 2022.
- [2] Kymeta corp. Link-budget calculations for a satellite link with an electronically steerable antenna terminal. Technical report, Kymeta corporation, 2019.
- [3] R.K. Crane. Prediction of the effects of rain on satellite communication systems. *Proceedings of the IEEE*, 65(3):456–474, 1977.
- [4] C. Daehnick, I. Klinghoffer, B. Maritz, and B. Wisem. Large leo satellite constellations: Will it be different this time? Technical report, McKensey & Company, May 2020.
- [5] Inigo del Portillo, Bruce G. Cameron, and Edward F. Crawley. A technical comparison of three low earth orbit satellite constellation systems to provide global broadband. *Acta Astronautica*, 159:123–135, 2019.
- [6] P. Delos, B. Broughton, and J. Kraft. Phased array antenna patterns—part 1: Linear array beam characteristics and array factor. Technical Report 2, Analog.com, 2020.
- [7] Yue Guan, Fan Geng, and Joseph Homer Saleh. Review of high throughput satellites: Market disruptions, affordability-throughput map, and the cost per bit/second decision tree. *IEEE Aerospace and Electronic Systems Magazine*, 34(5):64–80, 2019.
- [8] A. Guidotti, A. Vanelli-Coralli, M. Caus, J. Bas, G. Colavolpe, T. Foggi, S. Cioni, A. Modenini, and D. Tarchi. Satellite-enabled lte systems in leo constellations. In *2017 IEEE International Conference on Communications Workshops (ICC Workshops)*, pages 876–881, 2017.
- [9] Alessandro Guidotti, Alessandro Vanelli-Coralli, Matteo Conti, Stefano Andrenacci, Symeon Chatzinotas, Nicola Maturo, Barry Evans, Adegbenga Awoseyila, Alessandro Ugolini, Tommaso Foggi, Lorenzo Gaudio, Nader Alagha, and Stefano Cioni. Architectures and key technical challenges for 5g systems incorporating satellites. *IEEE Transactions on Vehicular Technology*, 68(3):2624–2639, 2019.
- [10] Mark Handley. Delay is not an option: Low latency routing in space. In *Proceedings of the 17th ACM Workshop on Hot Topics in Networks*, HotNets ’18, page 85–91, New York, NY, USA, 2018. Association for Computing Machinery.
- [11] Mark Handley. Using ground relays for low-latency wide-area routing in megaconstellations. In *Proceedings of the 18th ACM Workshop on Hot Topics in Networks*, HotNets ’19, page 125–132, New York, NY, USA, 2019. Association for Computing Machinery.
- [12] S. Victor Hum. Antenna arrays, radio and microwave wireless systems. Technical report, Univ. Toronto, Canada, 2020.
- [13] S. et al Jeux. Non-Terrestrial Networks position paper. Technical report, Next-Generation Mobile Networks Alliance, 2019.

- [14] Simon Kassing, Debopam Bhattacharjee, André Baptista Águas, Jens Eirik Saethre, and Ankit Singla. Exploring the "internet from space" with hypatia. In *Proceedings of the ACM Internet Measurement Conference, IMC '20*, page 214–229, New York, NY, USA, 2020. Association for Computing Machinery.
- [15] Oltjon Kodheli, Eva Lagunas, Nicola Maturo, Shree Krishna Sharma, Bhavani Shankar, Jesus Fabian Mendoza Montoya, Juan Carlos Merlano Duncan, Danilo Spano, Symeon Chatzinotas, Steven Kisseleff, Jorge Querol, Lei Lei, Thang X. Vu, and George Goussetis. Satellite communications in the new space era: A survey and future challenges. *IEEE Communications Surveys & Tutorials*, 23(1):70–109, 2021.
- [16] Oltjon Kodheli, Nicola Maturo, Stefano Andrenacci, Symeon Chatzinotas, and Frank Zimmer. Link budget analysis for satellite-based narrowband iot systems. In Maria Rita Palattella, Stefano Scanzio, and Sinem Coleri Ergen, editors, *Ad-Hoc, Mobile, and Wireless Networks*, pages 259–271, Cham, 2019. Springer International Publishing.
- [17] Kevin T. Li, Christian A. Hofmann, Harald Reder, and Andreas Knopp. A techno-economic assessment and tradespace exploration of low earth orbit mega-constellations. *IEEE Communications Magazine*, pages 1–7, 2022.
- [18] M. Mathis, J. Semke, J. Mahdavi, and T. Ott. The macroscopic behavior of the tcp congestion avoidance algorithm. *ACM SIGCOM Computer Communications Review*, 27(3):67–82, 1997.
- [19] Christopher McLain and Janet King. Future ku-band mobility satellites. In *35th AIAA International Communications Satellite Systems Conference*, 2017.
- [20] Jitendra Padhye, Victor Firoiu, Don Towsley, and Jim Kurose. Modeling tcp throughput: A simple model and its empirical validation. In *Proceedings of the ACM SIGCOMM '98 Conference on Applications, Technologies, Architectures, and Protocols for Computer Communication*, SIGCOMM '98, page 303–314, New York, NY, USA, 1998. Association for Computing Machinery.
- [21] Juan Rendon Schneir and Yupeng Xiong. Cost analysis of network sharing in ftt/pon. *IEEE Communications Magazine*, 52(8):126–134, 2014.
- [22] Federica Rinaldi, Helka-Liina Maattanen, Johan Torsner, Sara Pizzi, Sergey Andreev, Antonio Iera, Yevgeni Koucheryavy, and Giuseppe Araniti. Non-terrestrial networks in 5g & beyond: A survey. *IEEE Access*, 8:165178–165200, 2020.
- [23] Glenn Turner. Tcp performance. Technical report, Australia's Academic and Research Network, 2003.